

## Supporting information

### Real-Time Electron and Hole Transport Dynamics in Halide Perovskite Nanowires

Lisa Janker<sup>1,4</sup>, Yu Tong<sup>2</sup>, Lakshminarayana Polavarapu<sup>2,5</sup>, Jochen Feldmann<sup>2,4,5</sup>, Alexander S. Urban<sup>3,4,5,&</sup>, Hubert J. Krenner<sup>1,4,5,\*</sup>

<sup>1</sup> Lehrstuhl für Experimentalphysik 1 and Augsburg Centre for Innovative Technologies, Universität Augsburg, Universitätsstr. 1, 86179 Augsburg, Germany

<sup>2</sup> Chair for Photonics and Optoelectronics, Nano-Institute Munich, Department of Physics,

Ludwig-Maximilians-Universität München, Königinstr. 10, 80539 Munich, Germany

<sup>3</sup> Nanospectroscopy Group, Nano-Institute Munich, Department of Physics,

Ludwig-Maximilians-Universität München, Königinstr. 10, 80539 Munich, Germany

<sup>4</sup> Nanosystem Initiative Munich (NIM), Schellingstr. 4, 80339, Munich, Germany

<sup>5</sup> Center for Nanoscience (CeNS), Ludwig-Maximilians-Universität München, Geschwister-Scholl-Platz 1, 80539 Munich, Germany

\* Hubert Krenner: [hubert.krenner@physik.uni-augsburg.de](mailto:hubert.krenner@physik.uni-augsburg.de)

& Alexander Urban: [urban@lmu.de](mailto:urban@lmu.de)

Content:

1. Population decay analysis using a phenomenological model
2. Fourier analysis of PL transients
3. Model for numerical simulations of spatio-temporal carrier dynamics
4. Mobility analysis for a second NW bundle

### Population decay analysis using a phenomenological model

Our phenomenological model accounts for two effects on the charge carriers inside the NW induced by the SAW. The first effect is the polarization of the bound e-h pair at low electric fields. The second effect is the induction of spatio-temporal carrier dynamics. For the latter, in perovskites, the similar mobilities of electrons and holes lead to SAW-induced dynamics of both carrier species. This is in contrast to traditional semiconductors e.g. (In)GaAs, in which only the electrons are affected while the holes remain stationary. Both effects only depend on the direction of the SAW's electric field. This in turn leads to the observed  $T_{SAW}/2$ -periodic modulation. Thus, we assume that each decay rate contributing to the observed transients can be described by

$$\Gamma_i(t) = \Gamma_{i,0} - \Delta_i \cdot \sin^2(\omega_{SAW}t) \quad \text{Equation S1}$$

In this expression  $\Gamma_{i,0}$  denotes the native decay rate  $i$ , when neglecting the SAW-induced oscillations.  $\Delta_i$  is the amplitude of the intensity modulation. Thus, the full time-modulated transient can be written as

$$I(t) = \sum_{i=1}^3 A_i \cdot \exp(-\Gamma_{i,0}t) \cdot \exp(\Delta_i \cdot \sin^2(\omega_{SAW}t) \cdot t) \quad \text{Equation S2}$$

Finally, the total population decay rate is given by

$$\Gamma_{tot} = \sum_{i=1}^3 \Gamma_{i,0} - \Delta_i \quad \text{Equation S3}$$

Figure S1 shows the best fit of Equation S2 (red line, also shown in Figure 1c of the main manuscript) to the data (symbols) discussed in the main paper. The green line shows the extracted population decay  $N_{excitons}(t) = \sum_{i=1}^3 A_i \cdot \exp(-(\Gamma_{i,0} - \Delta_i) \cdot t)$ . We determine the mean number of excitons per NW from the number of photons absorbed by the NW bundle using the bulk absorption coefficient. The number of NWs in the bundle is estimated by scanning electron microscopy.

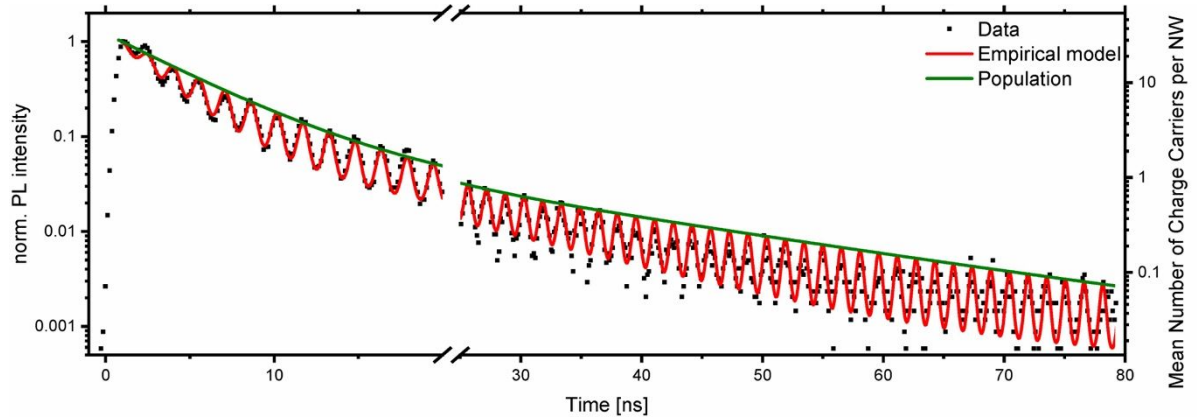


**Figure S1 – Population decay from phenomenological model – Fit of Equation S2 (red line) to the experimental data (symbols) and extracted population decay.**

Clearly our simple, phenomenological model describes the data over all times. However, it does not allow to draw conclusions on the underlying mechanism, which require the full model discussed in the main paper.

### Fourier analysis of PL transients

Figure S2 shows the Fast Fourier Transform (FFT) of the three PL transients recorded for the parallel SAW (Figure 2 a, black line), perpendicular SAW (Figure 2b, blue line) and both SAWs (Figure 2c, red line). Clearly no signatures are resolved for the perpendicular configuration because no SAW-driven dynamics occur. The FFT of the other two transients are nearly identical. This proves that the presence of the perpendicular SAW does not have any impact. In particular, it excludes that an exciton polarization by the perpendicular SAW's electric field would increase the dissociation by the parallel one. Furthermore, carriers, which are dissociated by the parallel SAW, are not transferred between NWs by the perpendicular one.

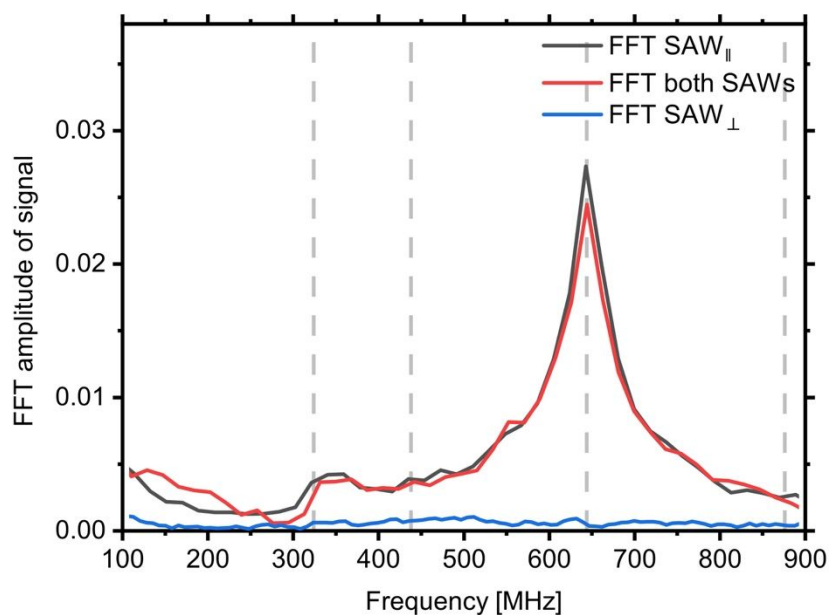


**Figure S2 – Fourier analysis of PL transients** – The same analysis shown in Figure 2d of the main paper was performed on the other transients.

### ***Numerical simulation of spatio-temporal carrier dynamics***

The SAW-driven spatiotemporal carrier dynamics were calculated using our chargeDynamics code<sup>1</sup> based on a model developed by Garcia-Cristobal and coworkers<sup>2</sup>. Further details can be found in references<sup>1,3</sup>. For the work presented here, the original code was extended to account for the multi-exponential PL decay observed for the unperturbed NWs as follows.

In order to account for the observed tri-exponential decay of the unperturbed NW emission, we included this process in the equations describing the SAW-driven spatio-temporal carrier dynamics. The modified equations are:

$$\frac{\partial n}{\partial t} = D_n \frac{\partial^2 n}{\partial x^2} + \mu_n E_x \frac{\partial n}{\partial x} + G + T - c \cdot np$$

$$\frac{\partial p}{\partial t} = D_p \frac{\partial^2 p}{\partial x^2} - \mu_p E_x \frac{\partial p}{\partial x} + G + T - c \cdot np$$

$$\frac{\partial X}{\partial t} = D_X \frac{\partial^2 X}{\partial x^2} - \frac{X}{\tau_1} - \frac{X}{\tau_2} - \frac{X}{\tau_3} - T + c \cdot np$$

For details on the model, readers are referred to original work detailing on the model.<sup>1-4</sup> Key parameters used in simulations relevant here are the length of the nanowire, which was set to 840 nm and the exciton binding energy defining the dissociation rate  $T$ , which was 20 meV.<sup>5,6</sup>

### Mobility analysis for a second NW bundle

We performed an analogous analysis on a second NW bundle following the same procedure described in the main paper. This analysis is presented in Figure S3. It follows the same procedure as the one presented in Figure 3 of the main text. For this NW bundle we obtain  $\mu_e = \mu_h = 4 \text{ cm}^2 \text{V}^{-1} \text{s}^{-1}$ , which corroborates the order of magnitude of the mobilities and that the mobility of electron and hole are equal.

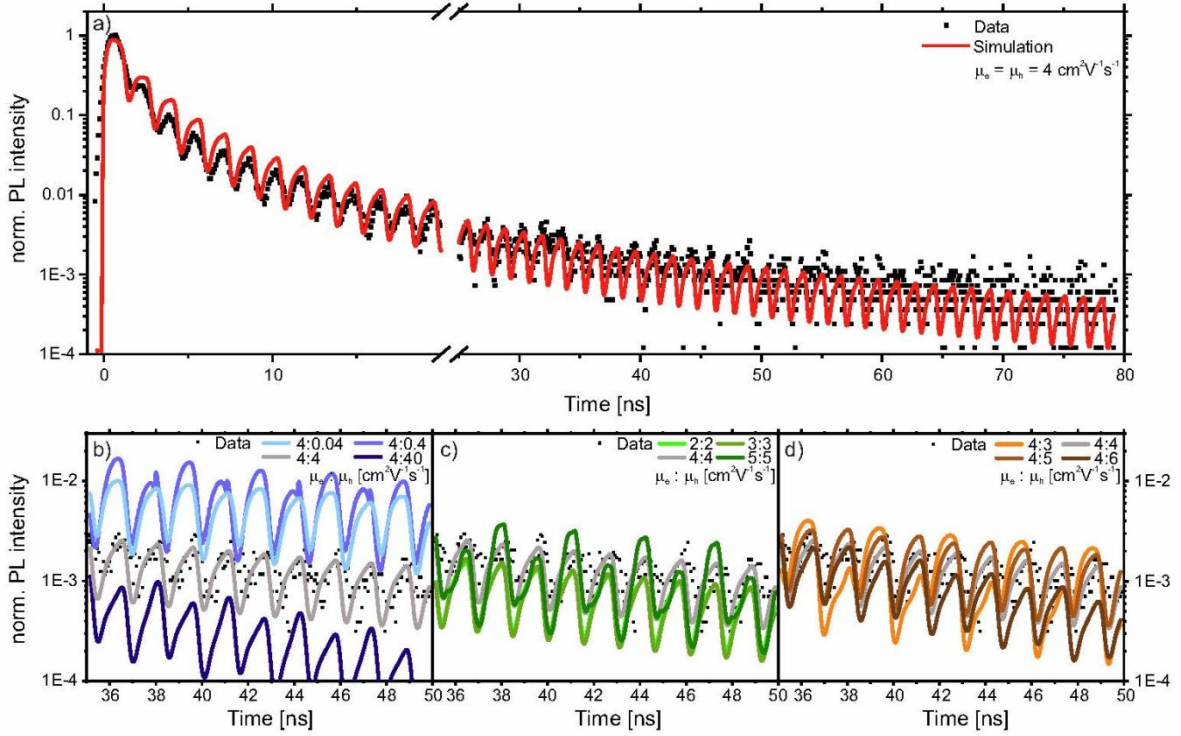


**Figure S3 – Mobility analysis of a second NW bundle** – The same analysis shown in Figure 3 of the main paper was performed on the data of another NW bundle and is presented here. (a) Experimentally observed SAW-modulated PL transient (symbols). Transient numerically derived from the SAW-driven spatio-temporal carrier dynamics for  $\mu_e = \mu_h = 4 \text{ cm}^2 \text{V}^{-1} \text{s}^{-1}$  (red line). (b-c) Detailed comparison of calculated transients (lines) for different values of  $\mu_e$  and  $\mu_h$  to the experimental data (symbols). In (b) the order of magnitude of the ratio between  $\mu_e$  and  $\mu_h$  is determined. (c) assumes a ratio of 1 and varies the value. Finally, (d) confirms  $\mu_e = \mu_h$ .

### ***Supplementary references***

1. Kinzel, J. B. *et al.* The Native Material Limit of Electron and Hole Mobilities in Semiconductor Nanowires. *ACS Nano* **10**, 4942–4953 (2016).
2. García-Cristóbal, A., Cantarero, A., Alsina, F. & Santos, P. V. Spatiotemporal carrier dynamics in quantum wells under surface acoustic waves. *Phys. Rev. B* **69**, 205301 (2004).
3. Schülein, F. J. R. *et al.* Surface acoustic wave controlled charge dynamics in a thin InGaAs quantum well. *JETP Lett.* **95**, 575–580 (2012).
4. Schülein, F. J. R. *et al.* Acoustically regulated carrier injection into a single optically active quantum dot. *Phys. Rev. B* **88**, 085307 (2013).
5. Protesescu, L. *et al.* Nanocrystals of Cesium Lead Halide Perovskites (CsPbX<sub>3</sub>, X = Cl, Br, and I): Novel Optoelectronic Materials Showing Bright Emission with Wide Color Gamut. *Nano Lett.* **15**, 3692–3696 (2015).
6. Diroll, B. T., Zhou, H. & Schaller, R. D. Low-Temperature Absorption, Photoluminescence, and Lifetime of CsPbX<sub>3</sub> (X = Cl, Br, I) Nanocrystals. *Adv. Funct. Mater.* **28**, 1800945 (2018).